

## The nuclear excitation rate for low-lying excited states in $^{237}\text{U}$ and $^{238}\text{U}$

G. D. Doolen

MS-220 Los Alamos Scientific Laboratory, P. O. Box 1663, Los Alamos, New Mexico 87545

(Received 28 March 1978)

The rate at which the first nuclear excited state becomes populated is calculated as a function of temperature up to 30 keV for compressions from 0.3 times normal density to 100 times normal density for  $^{237}\text{U}$ . Detailed results are also presented for  $^{238}\text{U}$ . The deexcitation rates are shown to change by several orders of magnitude and the excitation rates are shown to be in the order of several percent per nanosecond at high temperatures and compressions.

[NUCLEAR REACTIONS Electron and photon induced reactions;  $^{237}\text{U}$  and  $^{238}\text{U}$  first excited states, lifetimes and internal conversion coefficients calculated, temperatures up to 30 keV and compression up to 100 times normal density.]

### INTRODUCTION

Because nuclear excited states have cross sections for various processes which often differ considerably from the ground state,<sup>1</sup> it is important to properly account for the nuclear excited states when treating problems such as neutron transport, transmutation of nuclei, and perhaps  $s$  processes in a supernova where temperatures of several keV are encountered. If the time scale of a process is of the order of nanoseconds, the question arises as to how rapidly the nuclear excited states reach their thermal equilibrium populations. The corresponding excitation rate has been calculated for several nuclei and the results for two uranium isotopes are presented here.

When a nucleus in its ground state is placed in a high-temperature environment, the excited states of the nucleus approach an equilibrium population whose ratio to the ground state population is given by the Boltzmann factor,

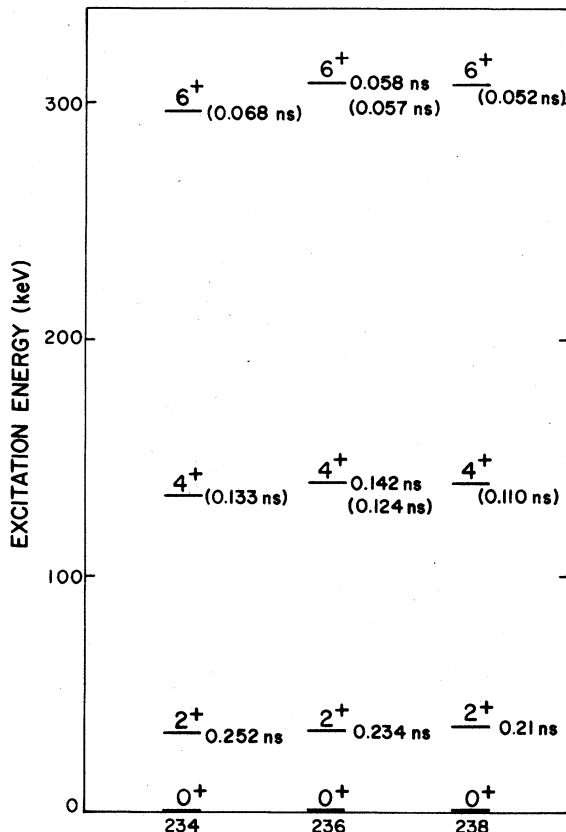
$$\frac{(2J_i + 1)e^{-E_i/kT}}{(2J_0 + 1)}, \quad (1)$$

where  $J_i$  and  $J_0$  are the spins of the  $i$ th excited state and the ground state, respectively,  $E_i$  is the energy of the excited state above the ground state,  $T$  is the temperature, and  $k$  is the Boltzmann constant.

To orient the reader to the excited state levels in uranium, these levels are plotted in Fig. 1 for three uranium isotopes with an even number of neutrons and protons. These nuclei exhibit rotational bands of excited states having spins of  $2^+$ ,  $4^+$ ,  $6^+$ , ... The half-lives without parentheses in Fig. 1 are taken from the Nuclear Data Tables. The half-lives with parentheses have been calculated using an ideal rotator model with an estimated uncertainty of less than 20%. It is evident that these even-even nuclei are similar. The re-

sults presented below for  $^{238}\text{U}$  can be considered to be characteristic of all even-even uranium isotopes.

Figure 2 shows the low-lying excited states of



### URANIUM ATOMIC NUMBER

FIG. 1. Low-lying excited states for three even-even uranium isotopes. The spin of each excited state is indicated. The excited state half-lives without parentheses are taken from Nuclear Data Tables. The half-lives in parentheses are calculated using the rotational model.

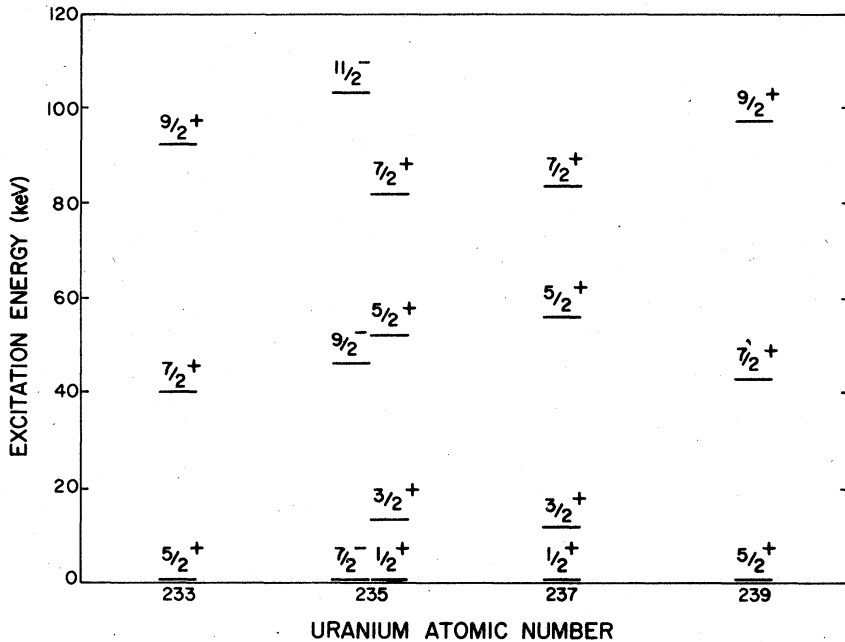


FIG. 2. Low-lying excited states for four odd- $A$  uranium isotopes.

the odd- $A$  isotopes of uranium. Each nucleus must be treated separately. Many of the excited states decay via  $M1$  transitions and their half-lives if not known experimentally must be calculated by incorporating single particle effects.

As an example of an odd- $A$  uranium nucleus, we shall present excitation rate results for  $^{237}\text{U}$ . The  $^{237}\text{U}$  results should not be considered characteristic of the odd- $A$  uranium nuclei, however, because the 11.5-keV excited state is lower than the  $^{233}\text{U}$  and  $^{239}\text{U}$  first excited states. The 11.5-keV energy of the  $^{237}\text{U}$  first excited state is less than the  $L$ -shell binding energy.

The fractions of nuclei in their excited states at equilibrium, calculated from Eq. (1), are presented in Fig. 3 as a function of temperature for  $^{238}\text{U}$  and  $^{237}\text{U}$ . This graph illustrates the fact that a significant fraction of the nuclei are excited when thermal equilibrium is reached. We shall now examine the rate at which this equilibrium population is approached.

#### NUCLEAR DECAY RATE AND ITS MODIFICATION FOR HIGH TEMPERATURES

Two physical processes dominate the nuclear excitation rate. One process is radiation excitation in which a photon from the blackbody spectrum is absorbed by the nucleus. The radiation excitation depends on the radiation temperature and the nuclear wave functions for the two states involved in the transition. The other process is inverse in-

ternal conversion, in which an electron in the continuum or an excited state makes the transition to a lower energy state and gives its transition energy to the nucleus. The inverse internal conversion

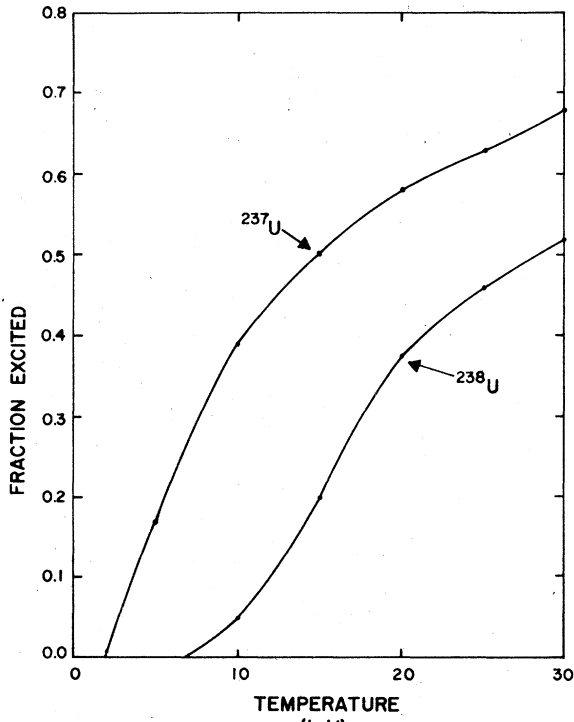


FIG. 3. The equilibrium fraction of nuclei in an excited state as a function of temperature for  $^{237}\text{U}$  and  $^{238}\text{U}$ .

process in addition depends on the electronic wave functions, which are sensitive to compression as well as temperature. First we shall discuss the nuclear decay rate and then relate it to the exci-

$$T_{J_i \rightarrow J_f} = 8\pi \sum_{\pi, L \geq 1} \left[ \left( \frac{\omega^{2L+1}(L+1)}{L[(2L+1)!!]} |\gamma(\pi, L, J_i \rightarrow J_f)|^2 \right) \left( 1 + \sum_{n,k} \alpha_{nk}(\pi L) \right) \right] + \sum_{nk} |e_{kn}(E0, J_i \rightarrow J_f)|^2, \quad (2)$$

Here  $\omega$  is the nuclear transition energy.  $|\gamma(\pi L, J_i \rightarrow J_f)|^2$  is the reduced transition probability (which contains the nuclear information),  $\pi$  and  $L$  are the parity and angular momentum of the transition, and  $J_i$  and  $J_f$  are the spins of the initial and final nuclear states.

The term  $\alpha_{nk}(\pi, L)$  is the internal conversion coefficient (which contains atomic electron information). The atomic orbital is specified by  $n$ , the principal quantum number, and by  $k$ , the total angular momentum quantum number.

The term  $|e_{kn}(E0, J_i \rightarrow J_f)|^2$  is the contribution to the transition probability from electric monopole transitions. Since electric monopole transitions are forbidden between nuclear states with different spin and since all transitions of interest here involve states with different spin, this term does not contribute to the transition rates.

The term 1, in

$$\left( 1 + \sum_{n,k} \alpha_{nk} \right),$$

is associated with a purely radiative transition.

Equation (2) requires modification when the atom is in equilibrium with a blackbody radiation field and an electron field at temperature  $T$ .

First, we note that the nuclear matrix element,  $\gamma(\pi, L, J_i \rightarrow J_f)$ , which depends on the expectation value of a nuclear operator between nuclear wave functions, is not significantly affected by the temperatures or compressions considered here.

Second, the radiative term, 1, is replaced by the term  $n+1$ , where  $n$  is the number of photons in the sample with energy equal to the difference in energy between the initial state,  $J_i$ , and the final state,  $J_f$ . Since  $n$  is positive this factor always enhances the transition probability and decreases the half-life.

Third, the term containing the internal conversion coefficients becomes modified. The original sum,

$$\sum_{n,k} \alpha_{nk},$$

describes the bound-free electron transition in which a bound electron is ejected into the continuum. At high temperatures, the bound states have a probability less than 1 of being occupied.

tation rate.

The total nuclear transition rate (excluding pair production, etc.) for decay of a nuclear excited state is<sup>2</sup>

We call this probability  $P_{nk}$ . The energy state into which the bound electron is ejected also has a finite probability of being occupied. We call this probability  $P_k$ . Because of the Pauli exclusion principle, which forbids two electrons with the same quantum numbers, we must multiply  $\alpha_{nk}$  by the probability of the final state being empty,  $1 - P_k$ . Hence the original sum,

$$\sum_{n,k} \alpha_{nk},$$

becomes

$$\sum_{n,k} \alpha'_{nk} P_{nk} (1 - P_k). \quad (3)$$

We place a prime on the  $\alpha$  because the electronic bound and continuum wave functions depend upon the compression and temperature. The calculation of the modified  $\alpha$ 's will be described below.

Fourth, two new types of terms arise which are added to the sum denoted in Eq. (3). Physically these terms are due to free-free and bound-bound electronic transitions. The free-free-transitions correspond to the excitation of continuum electrons to energies which are higher than the original energies by an amount equal to the energy of the nuclear transition. New bound-bound transitions can appear because the energy difference between atomic orbitals varies with temperature and compressions. A nuclear transition whose energy coincides with the energy difference between two atomic orbitals then becomes an allowed transition.

#### RELATION OF THE DECAY RATE TO THE EXCITATION RATE

At thermal equilibrium, the population of a given state is independent of time. The rate at which nuclei make transitions to a particular state equals the rate at which nuclei leave that excited state. Equation (2) gives the rate at which a nucleus will decay from a particular state with spin  $J_i$  to a lower energy state with spin  $J_f$ .

Consider a two-state nucleus and suppose at an equilibrium temperature  $T$  we have  $N_0$  such nuclei in the ground state and  $N_1$  such nuclei in the excited

TABLE I.  $\alpha$  for the 45-keV E2 transition in  $^{238}\text{U}$ . The notation  $A+n$  means  $A \times 10^n$ .

Shell	<i>T</i>	<i>C</i> = 0.3	<i>C</i> = 1.0	<i>C</i> = 3.0	<i>C</i> = 10	<i>C</i> = 30	<i>C</i> = 100
<i>L</i> I	0.05	8.01	8.01	8.01	8.02	8.01	7.98
	0.5	8.03	8.03	8.02	8.02	8.01	8.00
	1.0	8.07	8.06	8.05	8.05	8.02	8.04
	1.5	8.13	8.11	8.09	8.07	8.06	8.05
	2.0	8.21	8.16	8.13	8.11	8.09	8.06
	4.0	8.52	8.44	8.37	8.30	8.23	8.13
	7.0	8.95	8.82	8.72	8.59	8.47	8.33
	10.0	9.19	9.10	9.00	8.85	8.70	8.54
	20.0	9.64	9.49	9.40	9.33	9.22	9.00
	30.0	9.74	9.72	9.68	9.55	9.41	9.25
<i>L</i> II	0.05	2.35 +02	2.35 +02	2.35 +02	2.35 +02	2.35 +02	2.34 +02
	0.5	2.35 +02	2.35 +02	2.35 +02	2.35 +02	2.35 +02	2.34 +02
	1.0	2.36 +02	2.36 +02	2.36 +02	2.36 +02	2.35 +02	2.35 +02
	1.5	2.37 +02	2.37 +02	2.37 +02	2.36 +02	2.36 +02	2.35 +02
	2.0	2.39 +02	2.38 +02	2.37 +02	2.37 +02	2.36 +02	2.35 +02
	4.0	2.47 +02	2.45 +02	2.43 +02	2.41 +02	2.40 +02	2.38 +02
	7.0	2.58 +02	2.55 +02	2.52 +02	2.49 +02	2.46 +02	2.43 +02
	10.0	2.65 +02	2.62 +02	2.60 +02	2.55 +02	2.52 +02	2.48 +02
	20.0	2.78 +02	2.74 +02	2.71 +02	2.69 +02	2.66 +02	2.60 +02
	30.0	2.81 +02	2.80 +02	2.79 +02	2.76 +02	2.72 +02	2.67 +02
<i>L</i> III	0.05	2.07 +02	2.07 +02	2.07 +02	2.07 +02	2.07 +02	2.06 +02
	0.5	2.08 +02	2.08 +02	2.07 +02	2.07 +02	2.07 +02	2.06 +02
	1.0	2.09 +02	2.09 +02	2.08 +02	2.08 +02	2.08 +02	2.07 +02
	1.5	2.11 +02	2.10 +02	2.10 +02	2.09 +02	2.09 +02	2.08 +02
	2.0	2.13 +02	2.12 +02	2.11 +02	2.10 +02	2.10 +02	2.08 +02
	4.0	2.23 +02	2.21 +02	2.19 +02	2.16 +02	2.14 +02	2.11 +02
	7.0	2.35 +02	2.31 +02	2.29 +02	2.25 +02	2.22 +02	2.17 +02
	10.0	2.42 +02	2.39 +02	2.36 +02	2.32 +02	2.28 +02	2.23 +02
	20.0	2.54 +02	2.51 +02	2.47 +02	2.45 +02	2.43 +02	2.36 +02
	30.0	2.56 +02	2.55 +02	2.55 +02	2.52 +02	2.48 +02	2.43 +02
<i>M</i> I	0.05	2.38	2.37	2.38	2.38	2.36	2.13
	0.5	2.43	2.42	2.41	2.40	2.37	2.15
	1.0	2.54	2.51	2.49	2.46	2.42	2.23
	1.5	2.68	2.62	2.57	2.52	2.47	2.28
	2.0	2.81	2.74	2.68	2.60	2.52	2.33
	4.0	3.19	3.11	3.02	2.90	2.72	2.55
	7.0	3.44	3.38	3.30	3.18	3.04	2.84
	10.0	3.57	3.53	3.46	3.37	3.24	3.06
	20.0	3.78	3.72	3.67	3.62	3.54	3.42
	30.0	3.82	3.81	3.79	3.74	3.67	3.56
<i>M</i> II	0.05	6.26 +01	6.25 +01	6.27 +01	6.26 +01	6.23 +01	5.55 +01
	0.5	6.39 +01	6.37 +01	6.35 +01	6.32 +01	6.25 +01	5.63 +01
	1.0	6.68 +01	6.60 +01	6.54 +01	6.46 +01	6.38 +01	5.89 +01
	1.5	7.04 +01	6.90 +01	6.78 +01	6.64 +01	6.50 +01	6.02 +01
	2.0	7.38 +01	7.19 +01	7.04 +01	6.83 +01	6.64 +01	6.14 +01
	4.0	8.36 +01	8.15 +01	7.93 +01	7.63 +01	6.14 +01	6.69 +01
	7.0	8.96 +01	8.82 +01	8.61 +01	8.31 +01	7.05 +01	7.43 +01
	10.0	9.25 +01	9.14 +01	9.00 +01	8.77 +01	8.48 +01	7.99 +01
	20.0	9.75 +01	9.61 +01	9.47 +01	9.36 +01	9.16 +01	8.89 +01
	30.0	9.83 +01	9.82 +01	9.78 +01	9.66 +01	9.46 +01	9.25 +01
<i>M</i> III	0.05	5.80 +01	5.78 +01	5.80 +01	5.79 +01	5.73 +01	5.12 +01
	0.5	5.97 +01	5.94 +01	5.91 +01	5.87 +01	5.75 +01	5.17 +01
	1.0	6.32 +01	6.23 +01	6.15 +01	6.05 +01	5.92 +01	5.36 +01
	1.5	6.73 +01	6.57 +01	6.44 +01	6.26 +01	6.08 +01	5.53 +01
	2.0	7.13 +01	6.92 +01	6.73 +01	6.47 +01	6.23 +01	5.69 +01

TABLE I. (Continued)

Shell	<i>T</i>	<i>C</i> = 0.3	<i>C</i> = 1.0	<i>C</i> = 3.0	<i>C</i> = 10	<i>C</i> = 30	<i>C</i> = 100
<i>MIII</i>	4.0	8.18 +01	7.96 +01	7.72 +01	7.37 +01	6.84 +01	6.36 +01
	7.0	8.81 +01	8.66 +01	8.45 +01	8.13 +01	7.73 +01	7.17 +01
	10.0	9.10 +01	9.00 +01	8.84 +01	8.61 +01	8.31 +01	7.79 +01
	20.0	9.59 +01	9.46 +01	9.32 +01	9.20 +01	9.00 +01	8.70 +01
	30.0	9.65 +01	9.64 +01	9.61 +01	9.50 +01	9.31 +01	9.05 +01
	0.05	9.14 -01	9.11 -01	9.15 -01	9.14 -01	9.05 -01	7.52 -01
	0.5	9.49 -01	9.42 -01	9.37 -01	9.30 -01	9.12 -01	7.71 -01
	1.0	1.02	1.00	9.86 -01	9.67 -01	9.45 -01	8.35 -01
	1.5	1.11	1.03	1.04	1.01	9179 -01	8.68 -01
	2.0	1.21	1.16	1.11	1.06	1.0	8.98 -01
<i>MTIV</i>	4.0	1.54	1.46	1.39	1.29	1.16	1.04
	7.0	1.78	1.71	1.64	1.53	1.41	1.25
	10.0	1.88	1.85	1.79	1.70	1.58	1.42
	20.0	2.02	1.99	1.95	1.92	1.85	1.73
	30.0	2.04	2.03	2.03	2.00	1.95	1.86
<i>MV</i>	0.05	5.81 -01	5.79 -01	5.82 -01	5.81 -01	5.74 -01	4.76 -01
	0.5	6.04 -01	6.00 -01	5.96 -01	5.91 -01	5.79 -01	4.87 -01
	1.0	6.52 -01	6.39 -01	6.28 -01	6.15 -01	6.00 -01	5.27 -01
	1.5	7.13 -01	6.89 -01	6.69 -01	6.46 -01	6.23 -01	5.49 -01
	2.0	7.76 -01	7.42 -01	7.14 -01	6.79 -01	6.47 -01	5.69 -01
	4.0	9.72 -01	9.28 -01	8.83 -01	8.26 -01	6.43 -01	6.63 -01
	7.0	1.10	1.07	1.02	9.64 -01	8.92 -01	7.98 -01
	10.0	1.16	1.14	1.11	1.06	9.95 -01	8.95 -01
	20.0	1.22	1.21	1.19	1.17	1.14	1.07
	30.0	1.23	1.23	1.23	1.21	1.19	1.14

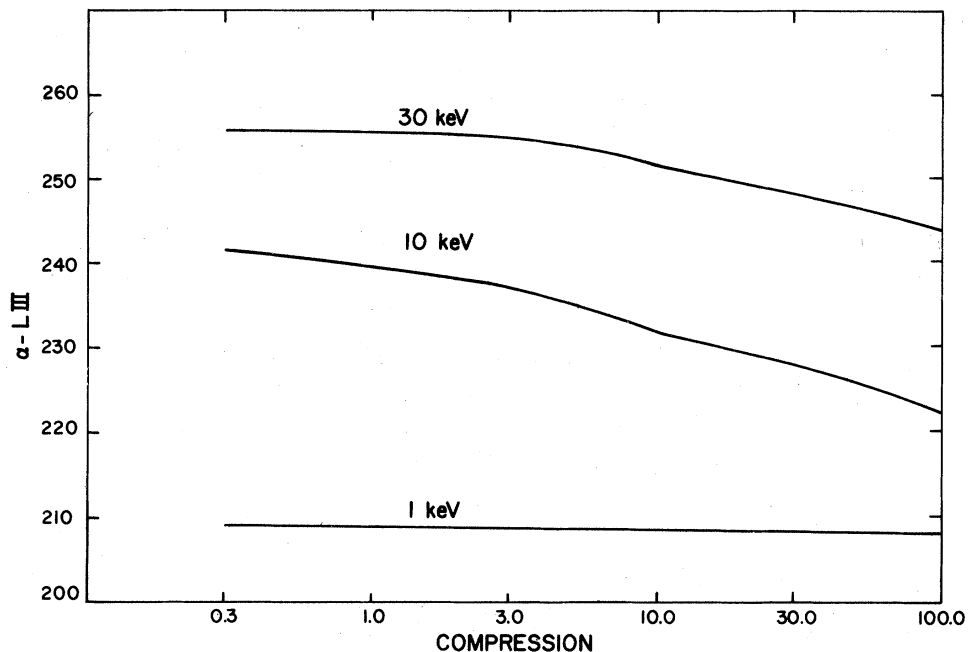


FIG. 4. The *L*III internal conversion coefficient for the 45-keV transition of  $^{238}\text{U}$  as a function of temperature and compression.

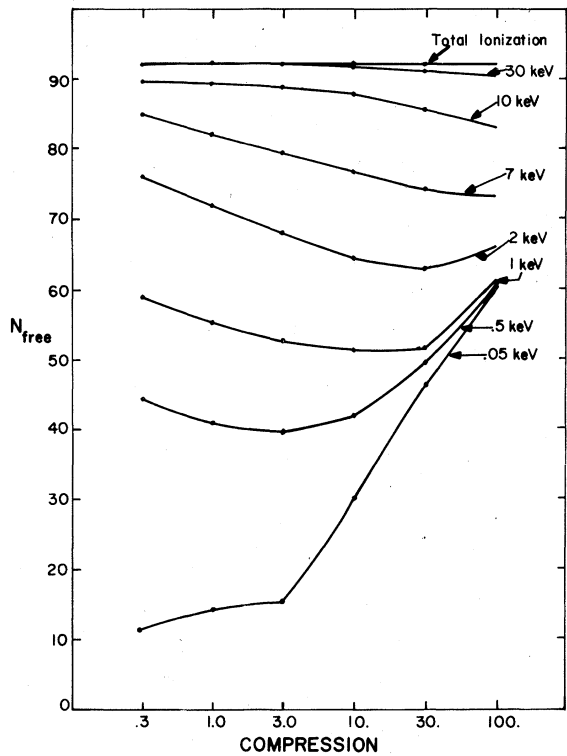


FIG. 5. The number of free electrons per uranium atom calculated as a function of temperature and compression from the Thomas-Fermi model.

state. For this system,

$$\frac{dN_0}{dt} = -N_1 T_{1 \rightarrow 0} - N_0 T_{0 \rightarrow 1},$$

$$\frac{dN_1}{dt} = N_1 T_{1 \rightarrow 0} + N_0 T_{0 \rightarrow 1}.$$

Here  $T_{i \rightarrow f}$  is the transition rate from state  $i$  to state  $f$ .

At equilibrium

$$\frac{dN}{dt} = 0$$

and

$$\frac{N_1}{N_0} = \frac{2J_1 + 1}{2J_0 + 1} e^{-E_i/kT}.$$

Hence,

$$T_{0 \rightarrow 1}^{\text{eq}} = \frac{N_1}{N_0} T_{1 \rightarrow 0}^{\text{eq}} = \frac{2J_1 + 1}{2J_0 + 1} e^{-E_i/kT} T_{1 \rightarrow 0}^{\text{eq}}, \quad (4)$$

where  $T_{i \rightarrow f}^{\text{eq}}$  is the equilibrium rate. If we assume that the electron and photon distributions are independent of the state of the nucleus, then  $T_{0 \rightarrow 1}^{\text{eq}}$  is independent of time. (This assumption concerning the electron and photon distributions requires that the photons and electrons at any energy are not

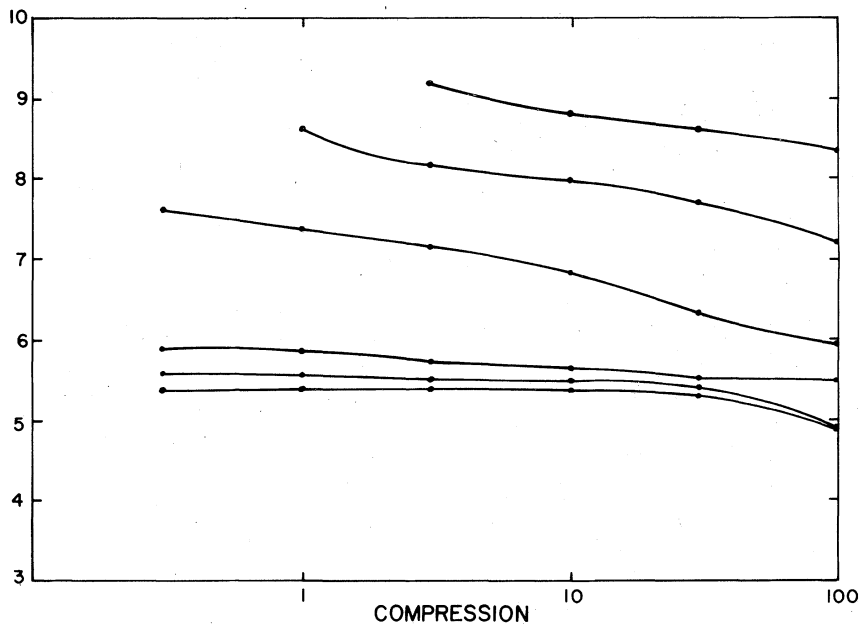


FIG. 6. The MIII internal conversion coefficient for the 11.5-keV transition of  $^{237}\text{U}$  as a function of temperature and compression.

TABLE II.  $\alpha$  for the 11.5-keV E2 and M1 transitions in  $^{237}\text{U}$ .

Shell multipole	$T$	$C = 1.0$	$C = 3.0$	$C = 10$	$C = 10$	$C = 30$	$C = 100$
<i>M1</i>	0.05	9.41 +02	9.40 +02	9.45 +02	9.50 +02	9.53 +02	8.79 +02
	0.5	9.67 +02	9.65 +02	9.65 +02	9.66 +02	9.63 +02	8.86 +02
	1.0	1.01 +03	1.00 +03	9.97 +02	9.88 +02	9.84 +02	9.13 +02
	1.5	1.07 +03	1.05 +03	1.04 +03	1.02 +03	1.01 +03	9.38 +02
	2.0	1.13 +03	1.10 +03	1.08 +03	1.06 +03	1.03 +03	9.63 +02
	4.0	0	0	1.24 +03	1.20 +03	1.12 +03	1.07 +03
	7.0	0	0	0	1.34 +03	1.28 +03	1.21 +03
	10.0	0	0	0	1.41 +03	1.38 +03	1.32 +03
	20.0	0	0	0	1.32 +03	1.52 +03	1.49 +03
	30.0	0	0	0	0	1.57 +03	1.55 +03
<i>E2</i>	0.05	4.78 +02	4.78 +02	4.78 +02	4.77 +02	4.75 +02	4.36 +02
	0.5	4.88 +02	4.86 +02	4.85 +02	4.84 +02	4.79 +02	4.39 +02
	1.0	5.08 +02	5.03 +02	4.97 +02	4.91 +02	4.87 +02	4.51 +02
	1.5	5.32 +02	5.23 +02	5.15 +02	5.06 +02	4.97 +02	4.60 +02
	2.0	5.55 +02	5.43 +02	5.32 +02	5.19 +02	5.05 +02	4.70 +02
	4.0	0	0	5.88 +02	5.70 +02	5.39 +02	5.11 +02
	7.0	0	0	0	6.11 +02	5.88 +02	5.57 +02
	10.0	0	0	0	6.29 +02	6.22 +02	5.92 +02
	20.0	0	0	0	7.65 +02	6.53 +02	6.41 +02
	30.0	0	0	0	0	6.65 +02	6.55 +02
<i>M1</i>	0.05	4.70 +04	4.69 +04	4.71 +04	4.70 +04	4.68 +04	4.23 +04
	0.5	4.81 +04	4.79 +04	4.77 +04	4.77 +04	4.73 +04	4.29 +04
	1.0	5.02 +04	4.97 +04	4.92 +04	4.85 +04	4.82 +04	4.45 +04
	1.5	5.28 +04	5.19 +04	5.11 +04	5.01 +04	4.92 +04	4.55 +04
	2.0	5.55 +04	5.41 +04	5.29 +04	5.15 +04	5.00 +04	4.64 +04
	4.0	0	6.24 +04	5.96 +04	5.73 +04	5.41 +04	5.07 +04
	7.0	0	0	0	6.24 +04	5.97 +04	5.62 +04
	10.0	0	0	0	6.54 +04	6.39 +04	6.01 +04
	20.0	0	0	0	7.07 +04	6.88 +04	6.70 +04
	30.0	0	0	0	0	7.09 +04	6.97 +04
<i>MII</i>	0.05	5.50 +01	5.49 +01	5.50 +01	5.50 +01	5.45 +01	4.94 +01
	0.5	5.62 +01	5.59 +01	5.58 +01	5.56 +01	5.50 +01	4.99 +01
	1.0	5.86 +01	5.80 +01	5.74 +01	5.66 +01	5.60 +01	5.16 +01
	1.5	6.17 +01	6.05 +01	5.96 +01	5.83 +01	5.74 +01	5.28 +01
	2.0	6.47 +01	6.31 +01	6.17 +01	6.02 +01	5.85 +01	5.40 +01
	4.0	0	7.01 +01	6.95 +01	6.69 +01	6.28 +01	5.90 +01
	7.0	0	0	0	7.26 +01	6.96 +01	6.54 +01
	10.0	0	0	0	7.62 +01	7.42 +01	7.00 +01
	20.0	0	0	0	9.61 +01	8.01 +01	7.79 +01
	30.0	0	0	0	0	8.21 +01	8.10 +01
<i>E2</i>	0.05	5.41 +04	5.40 +04	5.41 +04	5.40 +04	5.32 +04	4.82 +04
	0.5	5.56 +04	5.53 +04	5.51 +04	5.47 +04	5.36 +04	4.86 +04
	1.0	5.89 +04	5.80 +04	5.72 +04	5.63 +04	5.51 +04	4.99 +04
	1.5	6.27 +04	6.11 +04	5.99 +04	5.82 +04	5.68 +04	5.14 +04
	2.0	6.64 +04	6.43 +04	6.26 +04	6.04 +04	5.82 +04	5.30 +04
	4.0	7.59 +04	7.39 +04	7.16 +04	6.85 +04	6.37 +04	5.95 +04
	7.0	0	8.02 +04	7.83 +04	7.54 +04	7.19 +04	6.68 +04
	10.0	0	8.61 +04	8.17 +04	7.98 +04	7.70 +04	7.21 +04
	20.0	0	0	8.56 +04	8.51 +04	8.32 +04	8.06 +04
	30.0	0	0	9.16 +04	8.78 +04	8.61 +04	8.38 +04
<i>MIII</i>	0.05	3.37	3.37	3.37	3.37	3.32	3.01
	0.5	3.47	3.45	3.43	3.41	3.34	3.03
	1.0	3.67	3.61	3.56	3.50	3.44	3.12

TABLE II. (*Continued*)

Shell multipole	<i>T</i>	<i>C</i> = 0.3	<i>C</i> = 1.0	<i>C</i> = 3.0	<i>C</i> = 10	<i>C</i> = 30	<i>C</i> = 100
<i>MIII</i>	1.5	3.89	3.80	3.73	3.62	3.53	3.21
<i>M1</i>	2.0	4.11	3.99	3.88	3.75	3.61	3.31
	4.0	4.66	4.56	4.42	4.24	3.95	3.69
	7.0	0	4.91	4.81	4.63	4.43	4.12
	10.0	0	6.05	4.99	4.88	4.72	4.43
	20.0	0	0	5.21	5.17	5.06	4.92
	30.0	0	0	5.50	5.31	4.23	5.10
<i>MIV</i>	0.05	8.72 +02	8.69 +02	8.73 +02	8.72 +02	8.58 +02	7.19 +02
	0.5	9.03 +02	8.97 +02	8.92 +02	8.84 +02	8.66 +02	7.35 +02
	1.0	9.70 +02	9.52 +02	9.37 +02	9.17 +02	8.95 +02	7.90 +02
<i>E2</i>	1.5	1.05 +03	1.02 +03	9.93 +02	9.60 +02	9.30 +02	8.21 +02
	2.0	1.14 +03	1.09 +03	1.05 +03	1.01 +03	9.66 +02	8.49 +02
	4.0	1.43 +03	1.36 +03	1.29 +03	1.21 +03	1.09 +03	9.85 +02
	7.0	0	1.59 +03	1.52 +03	1.42 +03	1.32 +03	1.18 +03
	10.0	0	1.84 +03	1.65 +03	1.57 +03	1.47 +03	1.32 +03
	20.0	0	0	1.78 +03	1.77 +03	1.71 +03	1.60 +03
	30.0	0	0	1.90 +03	1.83 +03	1.79 +03	1.71 +03
<i>MIV</i>	0.05	6.10 -01	6.08 -01	6.10 -01	6.08 -01	5.96 -01	4.96 -01
	0.5	6.30 -01	6.26 -01	6.22 -01	6.15 -01	6.00 -01	5.06 -01
	1.0	6.75 -01	6.63 -01	6.52 -01	6.38 -01	6.19 -01	5.44 -01
<i>M1</i>	1.5	7.32 -01	7.09 -01	6.89 -01	6.65 -01	6.43 -01	5.64 -01
	2.0	7.91 -01	6.59 -01	7.31 -01	6.98 -01	6.67 -01	5.82 -01
	4.0	9.78 -01	9.35 -01	8.89 -01	8.35 -01	7.51 -01	6.73 -01
	7.0	0	1.07	1.03	9.68 -01	8.97 -01	8.01 -01
	10.0	0	1.26	1.11	1.06	9.94 -01	8.94 -01
	20.0	0	0	1.19	1.18	1.14	1.06
	30.0	0	0	1.27	1.22	1.19	1.13
<i>MV</i>	0.05	6.11 +02	6.09 +02	6.12 +02	6.10 +02	6.00 +02	5.03 +02
	0.5	6.33 +02	6.29 +02	6.25 +02	6.19 +02	6.06 +02	5.12 +02
	1.0	6.81 +02	6.67 +02	6.57 +02	6.43 +02	6.27 +02	5.48 +02
<i>E2</i>	1.5	7.39 +02	7.15 +02	6.96 +02	6.72 +02	6.50 +02	5.70 +02
	2.0	7.98 +02	7.65 +02	7.38 +02	7.06 +02	6.75 +02	5.91 +02
	4.0	9.80 +02	9.39 +02	8.97 +02	8.44 +02	7.61 +02	6.86 +02
	7.0	1.15 +03	1.07 +03	1.03 +03	9.74 +02	9.06 +02	8.16 +02
	10.0	0	1.14 +03	1.11 +03	1.06 +03	1.00 +03	9.08 +02
	20.0	0	2.80 +03	1.18 +03	1.17 +03	1.13 +03	1.07 +02
	30.0	0	0	1.22 +03	1.21 +03	1.18 +03	1.13 +02
<i>MV</i>	0.05	3.08 -01	3.07 -01	3.08 +01	3.06 -01	3.00 -01	2.49 -01
	0.5	3.19 -01	3.17 -01	3.14 +01	3.10 -01	3.03 -01	2.54 -01
	1.0	3.44 -01	3.36 -01	3.30 +01	3.23 -01	3.13 -01	2.72 -01
<i>M1</i>	1.5	3.73 -01	3.61 -01	3.50 +01	3.37 -01	3.25 -01	2.83 -01
	2.0	4.04 -01	3.86 -01	3.72 +01	3.55 -01	3.38 -01	2.93 -01
	4.0	5.00 -01	4.77 -01	4.54 +01	4.26 -01	3.82 -01	3.41 -01
	7.0	5.89 -01	5.48 -01	5.26 +01	4.93 -01	4.57 -01	4.08 -01
	10.0	0	5.85 -01	5.68 +01	5.39 -01	5.06 -01	4.55 -01
	20.0	0	1.61	6.07 +01	5.98 -01	5.78 -01	5.39 -01
	30.0	0	0	6.27 +01	6.18 -01	6.02 -01	5.72 -01
<i>NI</i>	0.05	2.89 +02	2.88 +02	2.89 +02	2.83 +02	2.61 +02	3.23 +02
	0.5	3.38 +02	3.29 +02	3.21 +02	3.03 +02	2.82 +02	3.25 +02
	1.0	4.07 +02	3.89 +02	3.72 +02	3.36 +02	3.15 +02	3.29 +02
<i>E2</i>	1.5	4.66 +02	4.29 +02	4.17 +02	3.76 +02	3.51 +02	3.45 +02
	2.0	5.10 +02	4.80 +02	4.39 +02	4.16 +02	3.87 +02	3.64 +02
	4.0	6.24 +02	6.01 +02	5.70 +02	5.28 +02	4.95 +02	4.34 +02
	7.0	6.91 +02	6.77 +02	6.59 +02	6.28 +02	5.88 +02	5.14 +02

TABLE II. (*Continued*)

Shell multipole	T	C = 0.3	C = 1.0	C = 3.0	C = 10	C = 30	C = 100
<i>N</i> I	10.0	7.22 +02	7.13 +02	6.98 +02	6.77 +02	6.45 +02	5.75 +02
<i>E</i> 2	20.0	7.66 +02	6.57 +02	7.47 +02	8.41 +02	7.17 +02	6.68 +02
	30.0	7.42 +02	7.75 +02	7.74 +02	7.66 +02	7.49 +02	7.04 +02
	0.05	1.32 +02	1.32 +02	1.31 +02	1.28 +02	1.17 +02	1.46 +02
	0.5	1.52 +02	1.49 +02	1.45 +02	1.36 +02	1.27 +02	1.47 +02
	1.0	1.81 +02	1.73 +02	1.65 +02	1.50 +02	1.40 +02	1.46 +02
<i>N</i> I	1.5	2.08 +02	1.88 +02	1.83 +02	1.66 +02	1.55 +02	1.53 +02
<i>M</i> 1	2.0	2.18 +02	2.06 +02	1.91 +02	1.81 +02	1.69 +02	1.60 +02
	4.0	2.52 +02	2.45 +02	2.35 +02	2.20 +02	2.09 +02	1.85 +02
	7.0	2.67 +02	2.64 +02	2.59 +02	2.49 +02	2.36 +02	2.09 +02
	10.0	2.74 +02	2.71 +02	2.67 +02	2.61 +02	2.51 +02	2.26 +02
	20.0	2.81 +02	2.79 +02	2.77 +02	3.11 +02	2.66 +02	2.50 +02
	30.0	2.83 +02	2.83 +02	2.82 +02	2.78 +02	2.73 +02	2.57 +02
	0.05	1.29 +04	1.28 +04	1.28 +04	1.25 +04	1.13 +04	1.45 +04
	0.5	1.51 +04	1.48 +04	1.43 +04	1.34 +04	1.23 +04	1.46 +04
	1.0	1.83 +04	1.74 +04	1.66 +04	1.49 +04	1.38 +04	1.45 +04
<i>N</i> II	1.5	2.08 +04	1.97 +04	1.86 +04	1.66 +04	1.54 +04	1.52 +04
<i>E</i> 2	2.0	2.26 +04	2.12 +04	2.01 +04	1.83 +04	1.69 +04	1.61 +04
	4.0	2.69 +04	2.60 +04	2.47 +04	2.29 +04	2.17 +04	1.90 +04
	7.0	2.91 +04	2.86 +04	2.78 +04	2.66 +04	2.50 +04	2.20 +04
	10.0	3.01 +04	2.97 +04	2.91 +04	2.83 +04	2.69 +04	2.40 +04
	20.0	3.17 +04	3.13 +04	3.08 +04	3.03 +04	2.94 +04	2.73 +04
	30.0	3.20 +04	3.20 +04	3.18 +04	3.14 +04	3.05 +04	2.86 +04
	0.05	1.50 +01	1.50 +01	1.49 +01	1.45 +01	1.32 +01	1.68 +01
	0.5	1.76 +01	1.72 +01	1.67 +01	1.56 +01	1.43 +01	1.69 +01
	1.0	2.13 +01	2.03 +01	1.93 +01	1.73 +01	1.60 +01	1.68 +01
<i>N</i> II	1.5	2.42 +01	2.29 +01	2.16 +01	1.94 +01	1.79 +01	1.77 +01
<i>M</i> 1	2.0	2.62 +01	2.47 +01	2.34 +01	2.13 +01	1.97 +01	1.86 +01
	4.0	3.11 +01	3.01 +01	2.87 +01	2.66 +01	2.51 +01	2.20 +01
	7.0	3.36 +01	3.31 +01	3.22 +01	3.08 +01	2.90 +01	2.55 +01
	10.0	3.47 +01	3.43 +01	3.36 +01	3.27 +01	3.11 +01	2.78 +01
	20.0	3.67 +01	3.61 +01	3.55 +01	3.49 +01	3.39 +01	3.15 +01
	30.0	3.70 +01	3.70 +01	3.67 +01	3.61 +01	3.51 +01	3.29 +01
	0.05	1.49 +04	1.48 +04	1.47 +04	1.40 +04	1.33 +04	1.66 +04
	0.5	1.82 +04	1.76 +04	1.69 +04	1.55 +04	1.48 +04	1.67 +04
	1.0	2.25 +04	2.13 +04	2.01 +04	1.78 +04	1.66 +04	1.68 +04
<i>N</i> III	1.5	2.58 +04	2.43 +04	2.27 +04	2.03 +04	1.88 +04	1.77 +04
<i>E</i> 2	2.0	2.81 +04	2.64 +04	2.47 +04	2.27 +04	2.09 +04	1.88 +04
	4.0	3.37 +04	3.25 +04	3.08 +04	2.85 +04	2.66 +04	2.26 +04
	7.0	3.65 +04	3.59 +04	3.49 +04	3.32 +04	3.10 +04	2.66 +04
	10.0	3.78 +04	3.73 +04	3.65 +04	3.54 +04	3.36 +04	2.94 +04
	20.0	3.98 +04	3.93 +04	3.86 +04	3.79 +04	3.66 +04	3.36 +04
	30.0	4.01 +04	4.01 +04	3.99 +04	3.93 +04	3.80 +04	3.51 +04
	0.05	9.15 - 01	9.10 - 01	9.02 - 01	8.61 - 01	8.17 - 01	1.02
	0.5	1.11	1.08	1.03	9.51 - 01	9.11 - 01	1.02
	1.0	1.37	1.30	1.23	1.09	1.01	1.03
<i>N</i> III	1.5	1.57	1.48	1.38	1.24	1.15	1.08
<i>M</i> 1	2.0	1.70	1.60	1.50	1.38	1.27	1.15
	4.0	2.02	1.95	1.86	1.72	1.61	1.37
	7.0	2.17	2.14	2.08	1.99	1.86	1.60
	10.0	2.24	2.21	2.17	2.11	2.01	1.76
	20.0	2.35	2.32	2.28	2.25	2.17	2.00
	30.0	2.36	2.36	2.35	2.32	2.24	2.08

TABLE II. (Continued)

Shell multipole	<i>T</i>	<i>C</i> = 0.3	<i>C</i> = 1.0	<i>C</i> = 3.0	<i>C</i> = 10	<i>C</i> = 30	<i>C</i> = 100
<i>NIV</i>	0.05	2.51 +02	2.49 +02	2.46 +02	2.32 +02	2.12 +02	2.90 +02
	0.5	3.26 +02	3.13 +02	2.97 +02	2.67 +02	2.42 +02	2.93 +02
	1.0	4.28 +02	4.01 +02	3.72 +02	3.20 +02	2.87 +02	2.94 +02
	1.5	5.16 +02	4.78 +02	4.39 +02	3.77 +02	3.36 +02	3.17 +02
	2.0	5.85 +02	5.36 +02	4.93 +02	4.32 +02	3.85 +02	3.45 +02
	<i>E2</i>	4.0	7.72 +02	7.30 +02	6.77 +02	6.03 +02	5.48 +02
	7.0	8.91 +02	8.61 +02	8.23 +02	7.66 +02	6.94 +02	5.70 +02
	10.0	9.44 +02	9.25 +02	8.94 +02	8.48 +02	7.82 +02	6.60 +02
	20.0	1.01 +03	9.97 +02	9.75 +02	9.51 +02	9.10 +02	8.12 +02
	30.0	1.02 +03	1.01 +03	1.01 +03	9.97 +02	9.61 +02	8.72 +02
<i>M1</i>	0.05	1.71 -01	1.69 -01	1.67 -01	1.57 -01	1.44 -01	1.97 -01
	0.5	2.21 -01	2.11 -01	2.01 -01	1.81 -01	1.64 -01	1.99 -01
	1.0	2.87 -01	2.69 -01	2.50 -01	2.15 -01	1.93 -01	1.99 -01
	1.5	3.43 -01	3.18 -01	2.93 -01	2.53 -01	2.25 -01	2.14 -01
	2.0	3.86 -01	3.54 -01	3.27 -01	2.88 -01	2.56 -01	2.32 -01
	<i>NIV</i>	4.0	4.96 -01	4.71 -01	4.39 -01	3.93 -01	3.60 -01
	7.0	5.64 -01	5.46 -01	5.24 -01	4.90 -01	4.46 -01	3.69 -01
	10.0	5.93 -01	5.82 -01	5.64 -01	5.37 -01	4.97 -01	4.23 -01
	20.0	6.29 -01	6.21 -01	6.08 -01	5.93 -01	5.68 -01	5.08 -01
	30.0	6.33 -01	6.31 -01	6.28 -01	6.18 -01	5.95 -01	5.41 -01
<i>NV</i>	0.05	1.65 +02	1.63 +02	1.61 +02	1.51 +02	1.41 +02	1.90 +02
	0.5	2.16 +02	2.07 +02	1.96 +02	1.75 +02	1.62 +02	1.92 +02
	1.0	2.82 +02	2.64 +02	2.45 +02	2.11 +02	1.90 +02	1.93 +02
	1.5	3.37 +02	3.13 +02	2.88 +02	2.49 +02	2.22 +02	2.09 +02
	2.0	3.78 +02	3.48 +02	3.21 +02	2.84 +02	2.54 +02	2.26 +02
	<i>E2</i>	4.0	4.84 +02	4.61 +02	4.30 +02	3.86 +02	3.55 +02
	7.0	5.48 +02	5.32 +02	5.11 +02	4.80 +02	4.38 +02	3.63 +02
	10.0	5.74 +02	5.64 +02	5.48 +02	5.24 +02	4.87 +02	4.14 +02
	20.0	6.06 +02	5.99 +02	5.88 +02	5.74 +02	5.53 +02	4.96 +02
	30.0	6.09 +02	6.08 +02	6.05 +02	5.98 +02	5.79 +02	5.27 +02
<i>M1</i>	0.05	8.53 -02	8.46 -02	8.31 -02	7.79 -02	7.27 -02	9.80 -02
	0.5	1.11 -01	1.07 -01	1.01 -01	9.05 -02	8.32 -02	9.90 -02
	1.0	1.46 -01	1.37 -01	1.27 -01	1.09 -01	9.79 -02	9.97 -02
	1.5	1.75 -01	1.62 -01	1.49 -01	1.28 -01	1.14 -01	1.07 -01
	<i>NV</i>	2.0	1.96 -01	1.80 -01	1.66 -01	1.46 -01	1.30 -01
	4.0	2.52 -01	2.40 -01	2.23 -01	2.00 -01	1.83 -01	1.49 -01
	7.0	2.85 -01	2.76 -01	2.65 -01	2.48 -01	2.26 -01	1.86 -01
	10.0	2.99 -01	2.94 -01	2.85 -01	2.71 -01	2.51 -01	2.13 -01
	20.0	3.18 -01	3.12 -01	3.05 -01	2.98 -01	2.86 -01	2.55 -01
	30.0	3.17 -01	3.16 -01	3.14 -01	3.10 -01	2.99 -01	2.71 -01

significantly depleted or enhanced by the nuclear decay or excitation processes. It can be argued that, by other scattering mechanisms, the electrons and photons are scattered so rapidly into and out of the energy regions affected by the decay and excitation processes that the equilibrium distributions are not significantly disturbed.)

#### CALCULATION OF THE TEMPERATURE AND COMPRESSION-DEPENDENT EXCITATION RATE

In order to calculate the excitation and deexcitation rates, a model for the electronic wave func-

tions must be adopted which describes their behavior at high temperatures and compressions. The model chosen here is a modified Thomas-Fermi model.<sup>3</sup> Briefly, the Dirac equation is solved in a Thomas-Fermi-type potential which goes to zero at the surface of an atomic sphere whose radius is determined by the compression. Compression is defined here as the factor by which one multiplies normal density to obtain the density of interest. The continuum is assumed to be depressed to  $E_0$ , the average of the potential seen by an electron over the atomic volume. The number of free electrons,  $N_f$ , is determined from

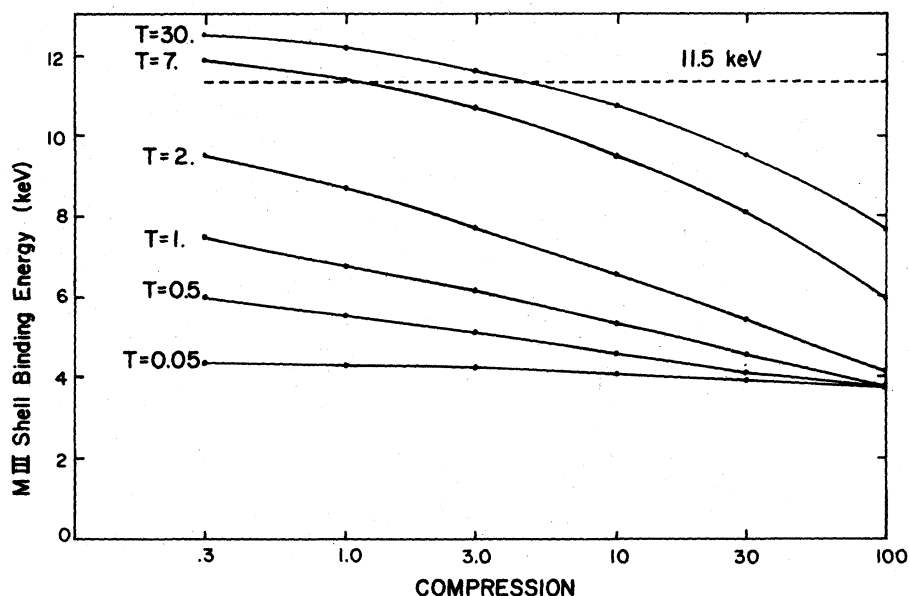


FIG. 7. The uranium MIII shell binding energy as a function of temperature and compression. The number labeling each curve is the temperature in keV.

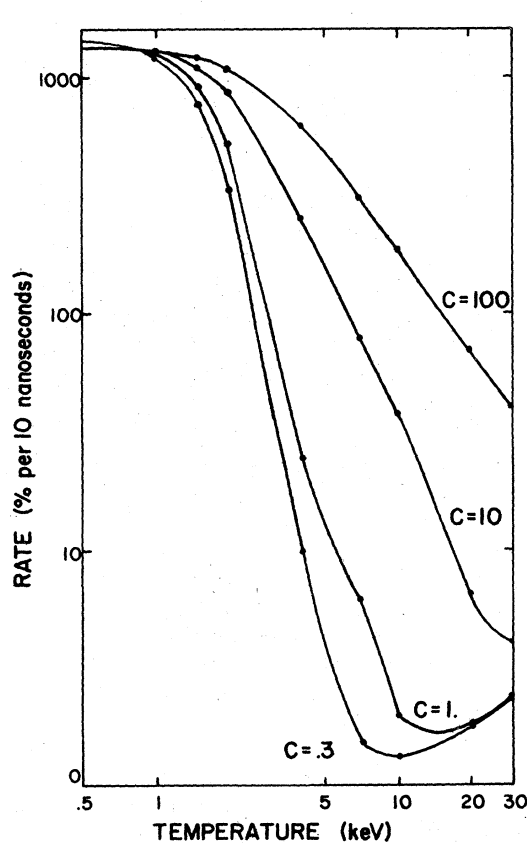


FIG. 8. The  $^{237}\text{U}$  bound-free plus radiative deexcitation rate from the  $\frac{3}{2}^+$  11.5-keV state to the  $\frac{1}{2}^+$  ground state.

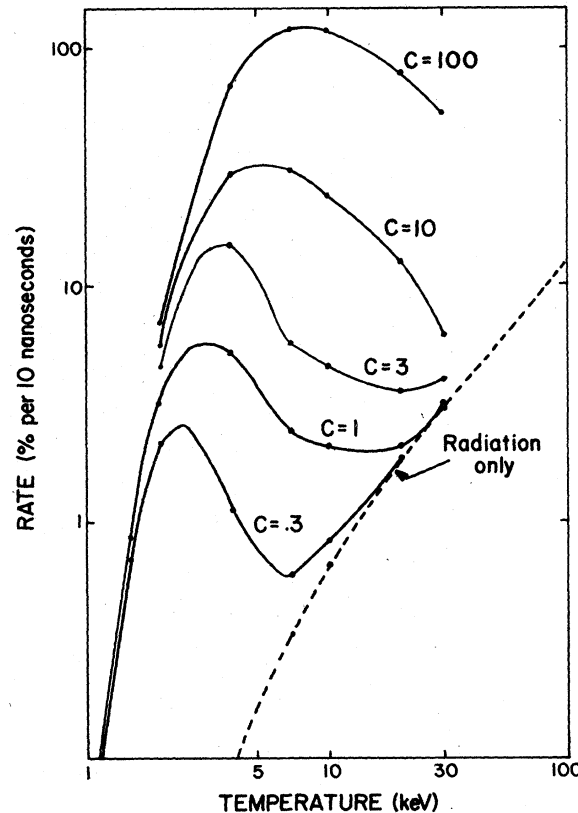


FIG. 9. The  $^{237}\text{U}$  free-bound plus radiative excitation rate from the  $\frac{1}{2}^+$  ground state to the  $\frac{3}{2}^+$  11.5-keV excited state.

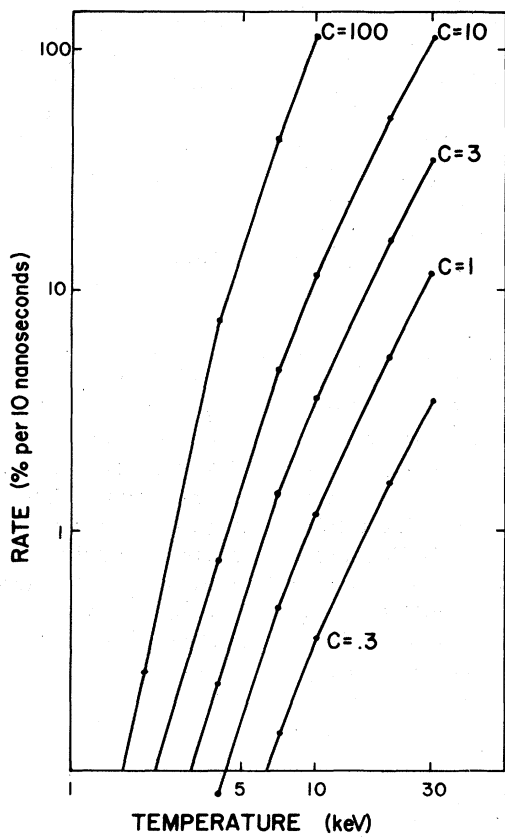


FIG. 10. The  $^{237}\text{U}$  free-free Born approximation excitation rate from the  $\frac{1}{2}^+$  ground state to the  $\frac{3}{2}^+$  11.5-keV excited state.

$$N_f = \frac{2}{3\pi} (kT)^{3/2} \left(\frac{r_0}{a_0}\right)^3 \int_0^\infty \frac{Z^{1/2} dZ}{1 + \exp[Z - (\mu + E_0)/kT]}.$$

This equation assumes a uniform continuum electron density. Here,  $r_0$  is the atomic sphere radius and  $a_0$  is the Bohr radius. The chemical potential,  $\mu$ , is determined by assuming a Fermi-Dirac distribution of all electrons and requiring neutrality of the atom, i.e.,  $Z = N_f + N_{\text{bound}}$ .

The program CATAR<sup>4</sup> was used with minor corrections to calculate the internal conversion coefficients. The coefficients related to the  $L\text{I}$ ,  $L\text{II}$ ,  $L\text{III}$ ,  $M\text{I}$ ,  $M\text{II}$ ,  $M\text{III}$ ,  $M\text{IV}$ ,  $M\text{V}$ , and  $N\text{I}$  shells were calculated at the temperatures 0.05, 0.5, 1.0, 1.5, 2.0, 4.0, 7.0, 10.0, 20.0, and 30.0 keV for compressions of 0.3, 1.0, 3.0, 10.0, 30.0, and 100. These coefficients are presented in Table I. In the table,  $A+n$  means  $A \times 10^n$ .

The corresponding variation of the  $L\text{III}$  internal conversion coefficient is presented in Fig. 4. This coefficient is one of the largest in the sum in Eq. (2). At high temperatures fewer electrons are bound so that an  $L\text{III}$  electron is shielded less from

the nucleus and is more tightly bound, making its wave function have more overlap with the nucleus. At the higher compressions more electrons are forced back into bound orbits causing greater shielding and decreasing the coefficient. The number of free electrons per uranium atom is plotted in Fig. 5 as a function of temperature and compression. The calculations were performed at compressions of 0.3, 1.0, 3.0, 10.0, 30.0, and 100.0. A free-hand curve was drawn between the points to connect points at the same temperature. If the points had been calculated correctly on a finer grid, there would have been a few oscillations at the lower temperatures due to shell structure.

The program CATAR was also used to calculate the  $M\text{I}$ ,  $M\text{II}$ ,  $M\text{III}$ ,  $M\text{IV}$ ,  $M\text{V}$ ,  $N\text{I}$ ,  $N\text{II}$ ,  $N\text{III}$ ,  $N\text{IV}$ , and  $N\text{V}$  internal conversion coefficients of the  $M\text{I}$  and  $E\text{2}$  components of the 11.5-keV transition in  $^{237}\text{U}$ . These coefficients, calculated as a function of temperature and compression, are presented in Table II. The corresponding variation of the  $M\text{III}$  internal conversion coefficient appears in Fig. 6. This coefficient is the largest for  $^{237}\text{U}$  except for high temperatures and low compressions where it vanishes because the binding energy of the  $M\text{III}$  level becomes greater than the transition energy of 11.5 keV. To illustrate this point, the binding energy of the  $M\text{III}$  shell is plotted in Fig. 7 as a function of temperature and compression. When the binding becomes greater than the 11.5-keV transition energy indicated in Fig. 7, the transition is not allowed in the atomic model used.

In the range of temperatures and compressions considered no bound-bound transitions were allowed for transition energies of 11.5 and 45 keV.

The free-bound excitation rate, the bound-free deexcitation rate, and the free-free excitation rate have been described previously<sup>5</sup> for  $^{238}\text{U}$ .

The bound-free deexcitation rate of the first excited 11.5-keV  $\frac{3}{2}^+$  state in  $^{237}\text{U}$  as calculated using the appropriately modified form of Eq. (2) is presented in Fig. 8. As in  $^{238}\text{U}$ , there is a rapid decrease in the rate by a few orders of magnitude, caused mostly by the change in the probability of occupation of the electronic orbits. In this calculation an  $E\text{2}/M\text{1}$  mixing ratio of 0.01 was assumed, as predicted by Bunker.  $B(E2\downarrow)$  was taken to be  $2.3 e^2 b^2$  and  $B(M1\downarrow)$  was taken to be

$$2.6 \times 10^{-2} \left(\frac{e\hbar}{2Mc}\right)^2,$$

as also predicted by Bunker.

The free-bound plus radiative rate from the  $\frac{1}{2}^+$  ground state to the first excited state in  $^{237}\text{U}$  is presented in Fig. 9 at compressions of 0.3, 1.0,

3.0, 10.0, and 100 times normal density. The radiative excitation rate, which is independent of compression, is also plotted separately. For all compressions considered there is a peak in the free-bound excitation rate caused by a maximum occurring in the number of electrons available at 11.5-keV above the electron-bound state energies.

The free-free contribution to the excitation rate, calculated in the Born approximation, is indicated in Fig. 10. Equation (6-55) in Eisenberg and Greiner was used for the differential cross section.<sup>6</sup> This cross section was multiplied by the appropriate initial and final state densities and Fermi-Dirac factors, and integrated over all angles and allowed energies. This rate dominates at higher temperatures. It is expected that the Born approximation is an underestimate of the actual free-free rate. Work is now in progress to calculate the free-free excitation rate using electron wave functions generated by a self-consistent atomic model.

#### CONCLUSION

It has been shown that the low-lying excited states of nuclei can approach their equilibrium

populations rapidly under extreme temperature and compression conditions and that the lifetime of these excited states can increase by several orders of magnitude. Because the excited states have neutron cross sections which differ from the ground state, it is important to properly account for the excited states.

#### ACKNOWLEDGMENTS

The author much appreciates valuable discussions with Walter Huebner in matters relating to the Thomas-Fermi potential, with Merle Bunker in matters relating to nuclear transition probabilities, and especially with David Liberman in matters relating to electronic transitions. The prediction of the  $E2/M1$  mixing ratio and the  $B(E2\downarrow)$  prediction by M. E. Bunker in a private communication is gratefully acknowledged. Some results contained herein were obtained using MACSYMA, a symbolic manipulation program developed at MIT and supported in part by the U. S. Department of Energy under Contract No. E(11-1)-3070 and by NASA under Grant No. NSG1323.

<sup>1</sup>D. G. Gardner, Lawrence Livermore Laboratory Report No. UCID-16885, 1975 (unpublished).

<sup>2</sup>H. C. Pauli, K. Alder, and R. M. Steffen, in *The Electromagnetic Interaction in Nuclear Spectroscopy*, edited by W. D. Hamilton (North-Holland, Amsterdam, 1975), pp. 26 and 360. Some misprints in the corresponding equation in the book are corrected here.

<sup>3</sup>R. Latter, Phys. Rev. 99, 1854 (1955).

<sup>4</sup>H. C. Pauli and U. Raff, Comput. Phys. Commun. 9, 392 (1975).

<sup>5</sup>G. D. Doolen Phys. Rev. Lett. 40, 1695 (1978).

<sup>6</sup>J. M. Eisenberg and W. Greiner, *Excitation Mechanisms of the Nucleus* (North-Holland, Amsterdam, 1970), p. 161.